JOURNAL OF ENGINEERING AND APPLIED SCIENCE, VOL. 67, NO. 1, Feb. 2020, PP. 1-30
FACULTY OF ENGINEERING, CAIRO UNIVERSITY

FRACTIONAL CALCULUS DEFINITIONS, APPROXIMATIONS, AND ENGINEERING APPLICATIONS

O. ELWY[1], A. M. ABDELATY[2], L. A. SAID[3], AND A. G. RADWAN[4,5]

ABSTRACT

The basic idea behind fractional calculus is that it considers derivatives and integrals of non-integer orders giving extra degrees of freedom and tuning knobs for modeling complex and memory dependent systems with compact descriptions. This paper reviews fractional calculus history, theory, and its applications in electrical engineering. The basic definitions of fractional calculus are presented together with some examples. Integer order transfer function approximations and constant phase elements (CPEs) emulators are overviewed due to their importance in implementing fractional-order circuits and controllers. The stability theory of fractional-order linear systems is outlined and discussed. Four common electrical engineering applications are surveyed. Fractional-order oscillators allow controlling the phase difference, as well as achieving high oscillation frequency independently. Fractional order electronic filters are used to provide non-integer order slopes eliminate the need to round up the filter order and achieve the exact required time and frequency domain specifications. Studying fractional-order bioimpedance models provides better fitting to the measured data from fruits and vegetables. Fractional order DC-DC converter models provide a better estimation of the power conversion efficiency by incorporating frequency-dependent losses.

KEYWORDS: Fractional-order Circuits, Caputo, Fractional Calculus, Cole-Impedance Model, DC-DC Converters, Filters, Oscillators.

1. INTRODUCTION

Gottfried Leibniz and Guillaume L'Hôpital are the first ones to wonder about the existence of the fractional order derivative in the end of the seventeenth century [1]. Since then, many great mathematicians had developed a strong theoretical foundations

[1]Research Assistant, Nanoelectronics Integrated Systems Center (NISC), Nile University, Egypt.
[2]Lecturer Assistant, Dept. of Engineering Mathematics and Physics, Fayoum University, Egypt.
[3]Assistant Professor, Nanoelectronics Integrated Systems Center (NISC), Nile University, Egypt.
[4]Professor, Engineering Mathematics and Physics Dept, Fac. of Engineering, Cairo University, Egypt.
[5]VP for Research, School of Engineering and Applied Sciences, Nile University, Giza, Egypt.

of the topic and, unfortunately, it remained within the boundaries of pure mathematics for a long time. The early contributors list include but not limited to: Leibniz, L'Hôpital, Bernoulli, Laplace, Euler, and Fourier [1]. Euler introduced the gamma function as a generalization of the factorial function and consequently generalized the formula of the n-th order derivative to the intermediate fractional orders. The first appearance of Riemann-Liouville fractional integrals and Caputo fractional derivative were presented in Abel's approach to solve the tautochrone problem. The systematic formulation of fractional calculus theory began with Liouville during the mid 19^{th} century followed by the contributions of Grunwald and Letnikov for the arbitrary order difference [1].

Fractional calculus and fractional-order modeling are areas of mathematics concerned with the treatment of the processes having non-integer differentiation and integration orders [2]. Despite the early start in developing the theoretical foundations of fractional calculus, it is only recently when researchers uncovered its strength in modeling many natural and complex phenomena. The application areas of fractional calculus and fractional-order modeling include but not limited to: control [3–6], chaotic systems [7–12], encryption [13–16], super-capacitor modeling [17–19] , filters [20–26], differentiators and integrators [27], and bioengineering [28–30].

The remaining of this review is organized as follows: Section 2 introduces the basic definitions of fractional calculus with some examples. Section 3 discusses various integer order approximation techniques for the fractional Laplacian operator while in Section 4, different circuit topologies of passive fractance emulators are discussed. The stability analysis concepts in the fractional domain are summarized in Section 5. Four electrical engineering applications of fractional calculus are summarized in Section 6 including oscillators, filters, bio-impedance, and DC-DC converters.

2. FRACTIONAL CALCULUS DEFINITIONS

Fractional calculus is the branch of mathematics that deals with non-integer order differentiation or integration. This gives the generality feature to the ordinary calculus. The n-fold integration of $f(t)$ can be calculated according to Cauchy's formula:

$D^{-n}f(t) = \frac{1}{(n-1)!}\int_0^t (t-\tau)^{n-1} f(\tau)d\tau$ [2]. Where D^- denotes the integration process and D^+ is the differentiation. This formula was generalized to a continuous one by Riemann and Liouville [2] using the continuous gamma function $\Gamma(\alpha)$ instead of the discrete factorial as follows:

$$D^{-\alpha} f(t) = \frac{1}{\Gamma(\alpha)} \int_0^t (t-\tau)^{\alpha-1} f(\tau)d\tau, \alpha > 0 \tag{1}$$

which is known as the Riemann-Liouville (RL) fractional integral. There are several definitions of the fractional differentiation such as RL, Caputo, and Grünwald-Letnikov (GL) [2, 31]. The fractional differentiation calculation in terms of an integer derivative and an RL fractional integral. The RL definition of the fractional derivative uses the ceil function to achieve that $D^{\alpha}_{RL} f(x) = D^{\lceil\alpha\rceil} D^{\lceil\alpha\rceil-\alpha} f(x)$. Then, The overall operation includes two sub-operations. The first one is fractional-order integration, and the second one is integer order differentiation. The general formula of RL definition of fractional derivative can be written as follows:

$${}^{RL}_{a}D^{\alpha}_{t} f(t) = \frac{1}{\Gamma(m-\alpha)} \left(\frac{d}{dt}\right)^m \int_a^t (t-\tau)^{m-\alpha-1} f(\tau)d\tau. \qquad (m-1 \leqslant \alpha < m) \tag{2}$$

This procedure results in non-integer order initial conditions which cannot be interpreted physically. The solution to this problem is the Caputo's definition of the fractional derivative, which depends on the same previous idea but with interchanging the positions of the integer differentiation and fractional integration. Caputo's definition is written as: $D^{\alpha}_{C} f(x) = D^{\lceil\alpha\rceil-\alpha} D^{\lceil\alpha\rceil} f(x)$, where the integer-order differentiation occurs first. The definition of Caputo is as follows:

$${}^{C}_{a}D^{\alpha}_{t} f(t) = \frac{1}{\Gamma(m-\alpha)} \int_a^t (t-\tau)^{m-\alpha-1} f^{(m)}(\tau)\, d\tau\,, \quad (m-1 < \alpha < m) \tag{3}$$

Caputo's definition uses initial conditions of the integer derivatives which can be physically measured. While, the RL definition uses the initial conditions of the fractional derivatives which have no physical meaning and cannot be measured. There is another

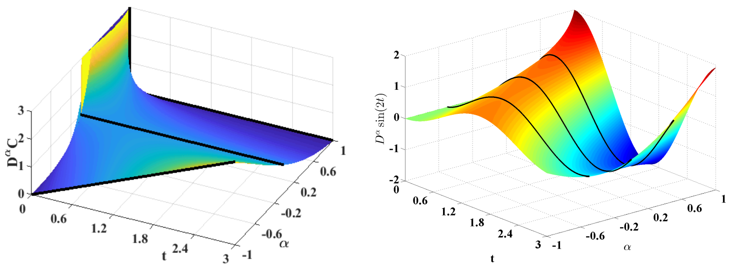

(a) (b)

Fig. 1. RL differ-integral of a constant (C) and b $f(t) = sin(2t)$.

difference with RL's definition, the constant differentiation. Caputo gives the ordinary answer by zero, while RL gives a solution as follows:

$$ {}^{RL}_{0}D^{\alpha}_{t}C = \frac{Ct^{-\alpha}}{\Gamma(1-\alpha)}, {}^{C}_{0}D^{\alpha}_{t}C = 0, \tag{4} $$

where C is the constant [2]. The RL differ-integral of a constant (C) and a sinusoid ($f(t) = sin(2t)$) for $-1 < \alpha < 1$ are illustrated in Fig. 1.

Grünwald-Letnikov (GL) definition is much similar to the definition of the classical n-th order derivative. There is a proven correspondence between GL and RL definitions [2]. For every ($0 < \alpha < n$), RL definition exists and coincides with GL definition, if $0 \leqslant m-1 \leqslant \alpha < m \leqslant n$. This equivalence occurs under the conditions:

1. The function $f(t)$ is $(n-1)$ times continuously differentiable in the targeted interval,

2. $f^{(n)}(t)$ is integrable in the targeted interval.

The GL derivative, in the interval $[a, t]$ is defined as follows:

$$ {}^{GL}_{a}D^{\alpha}_{t}f(t) = \lim_{h\to 0}\frac{1}{h^{\alpha}}\sum_{j=0}^{\lfloor (t-a)/h \rfloor}\omega^{(\alpha)}_{j}f(t-jh), \tag{5} $$

where $\omega^{(\alpha)}_{j}$ are the binomial coefficients, which can be calculated as: $\omega^{(\alpha)}_{j} = (1 - \frac{\alpha+1}{j})\omega^{(\alpha)}_{j-1}$, $\omega^{(\alpha)}_{0} = 1$, $j = 1, 2, 3, \ldots$. This approach gives the opportunity to use RL derivative during the problem formulation, and going back and forth to GL derivative to obtain numerical solutions. This definition is not interval bounded. Getting an accurate result requires the number of terms to be approaching to ∞, or at least to be a very large number.

3. INTEGER ORDER APPROXIMATION OF THE FRACTIONAL ORDER LAPLACIAN OPERATOR

The behavior of fractional linear systems is mimicked using either traditional integer transfer functions or digital filters. These approximations are important because [32]: commercial off-the-shelf constant phase elements are not available, reliable and well known simulation software are based on integer order calculus. So, having integer approximation of fractional order systems facilitates the use of these software tools, and synthesis of fractional order circuit is, in fact, based on integer transfer functions.

Discrete approximations of s^α can be converted into continuous approximations and continuous ones into discrete ones. Since digital approximations normally perform worse than continuous ones, the first alternative is seldom used.

Laplace transform is a mathematical operation that converts a function of a real variable (t) into a function of a complex variable (s). The Laplace transform of the any classical fractional derivative (F_1 class) under zero initial condition is [2, 31] :

$$\mathcal{L}\{{}_0D_t^\alpha f(t)\} = s^\alpha F(s), \tag{6}$$

which can be translated to a one-to-one correspondence between derivative term and the Laplacian operator ($\frac{d^\alpha}{dt^\alpha} \longleftrightarrow s^\alpha$), where $s = j\omega$. For the case of s^α, the magnitude is a linear line plotted with the logarithmic frequency axis as shown in Fig.2a. The phase angle has a single value forming a horizontal line as shown in Fig.2b. Both of the magnitude and phase obey the following equations:

$$Magnitude(s^\alpha) = 20\alpha\log(\omega), \quad Phase(s^\alpha) = \frac{\alpha\pi}{2}. \tag{7}$$

This property allows representing Laplacian operator-based transfer function using Bode diagrams [33]. They have two versions: one is the magnitude and the other is the phase angle. Both of these plots have logarithmic frequency x-axis. The magnitude and phase

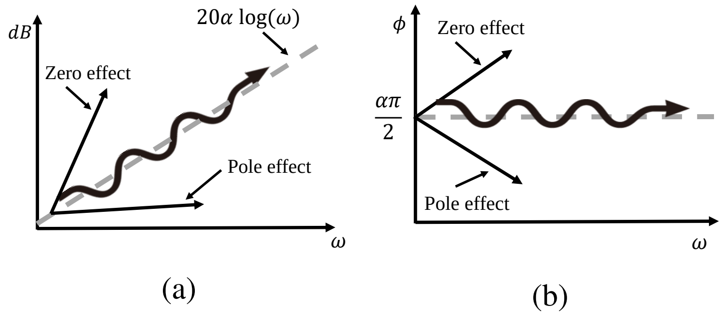

Fig. 2. Bode diagrams of s^{α} (a)Magnitude of s^{α} for any α and (b) Phase of s^{α} for any α.

are calculated for a given transfer function $H(j\omega)$ as follows:

$$H(j\omega) = \frac{z(j\omega)}{p(j\omega)}, \tag{8a}$$

$$Magnitude(H(j\omega)) = 20log|H(j\omega)|, \tag{8b}$$

$$phase(H(j\omega)) = \angle H(j\omega) = \tan^{-1}\left(\frac{Im\{H(j\omega)\}}{Re\{H(j\omega)\}}\right) = \angle z(j\omega) - \angle p(j\omega), \tag{8c}$$

where $z(j\omega)$, and $p(j\omega)$ are the zeros and poles of the transfer function respectively. Figure 2a and 2b show the effects of zeros and poles on the phase of a transfer function. Zero would take the phase angle higher, while pole would pull it down. The overall phase angle is the summation of these ups and downs as indicated in Eq. (8c). Because of the advances made on integer-order analysis, researchers tended to approximate s^{α} in terms of integer order s. The trick of integer order approximation techniques is to find a way to distribute/interlace the poles and zeros to obtain the desired response by zigzagging about the ideal fractional order response. The desired output should follow Eq. (7). Therefore, the approximation technique should try to find a representation that oscillates around $\alpha\pi/2$ using the angles' properties of poles and zeros. Also, the magnitude should preserve the presented relation in Eq. (7) and Fig.2a.

Many techniques were introduced to obtain distribution of zeros and poles. There are two categories of approximations according to [34]. The first category is named continued fraction expansions and interpolation techniques such as the approximations of Matsuda and Carlson. The second category is characterized by curve fitting and identification techniques such as Oustaloup. A summary of the design flow charts of four approximation techniques is provided in Table 1. The flowcharts show that all these approximation techniques provide control of the approximation order N and the fractional order α. However, only Oustaloup and Matsuda have the operating frequency range as their input parameters. Additionally, the effects of different parameters on each approximation are depicted in Table 2. For Carlson and CFE, the operating frequency range is enlarged by increasing N. While for Oustaloup and Matsuda, at a constant operating frequency range, the phase and magnitude errors decrease by increasing N. By varying α, it is evident that Carlson approximation is acceptable only at $\alpha = 0.5$.

4. FRACTIONAL-ORDER CAPACITOR EMULATORS

Resistors, capacitors, and inductors resemble the three basic circuit elements, and they are related through the formula $Z(s) = ks^{\alpha}$, where k is a coefficient that contributes to the impedance magnitude value and α is the order. for $\alpha = -1, 0, 1$, the relation represents the traditional capacitor, resistor, and inductor, respectively. Moreover, Frequency Dependent Negative Resistor (FDNR) [35] follow this generalized equation as shown in Fig. 3. Intermediate circuit elements appear in Fig.3 for non-integer values of α. These devices are called fractances or Constant Phase Elements (CPE), due to their nature of constant phase at $\alpha\pi/2$. The absence of off-the-shelf fractional order capacitors (FOC) encourages the researchers to find some alternatives. Many trials were introduced to emulate their behavior through either active or passive circuits.

Examples of passive CPE emulators are found in [36–38] while examples of active CPE emulators are found in [39–41]. Although active emulators allow more tunability, passive

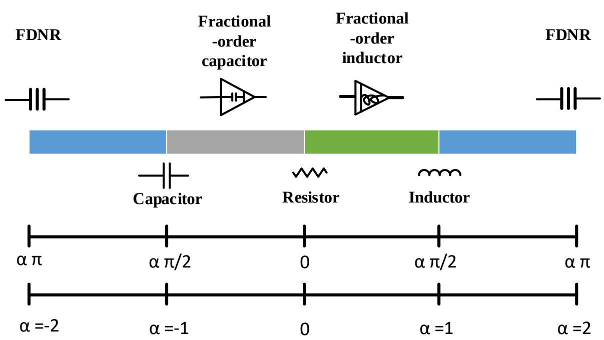

Fig. 3. Conventional elements and their relation to the fractional ones.

circuits based on RC networks are much cheaper. The passive emulators are obtained through two approaches, the first is a direct circuit approximation such as [36,38,42–44]. The second approach is through using integer order approximations of s^{α}, and converting them to a network of Lumped elements. The conversion can be done to yield circuits in the form of Foster-I, Foster-II, Cauer-I, or Cauer-II [45].

4.1 Emulators of $\alpha = 0.5$

The work of Roy [36] is one of the earliest approaches to build a circuit realization for FOC. Three different realizations were introduced, which are shown in Table 3. These designs are for approximating the order $\alpha = 0.5$ only.Later on, Nakagawa proposed another network [46]. Nakagawa employed the idea of the geometric mean to obtain a FOC's emulator in the shape of a self similar RC tree as shown in Table 3. Increasing the number of stages enlarges the operating frequency range, but it's not cost effective.

4.2 Generic Passive Emulators

Sugi proposed a network that emulates the behavior of FOC based on Distributed Relaxation Time models [37]. The current of a FOC can be expressed in terms of a superposition decay processes. The proposed two topologies are shown in Table 3. Valsa proposed another methodology [38, 44], and the networks are shown in Table 3. This method is analogous to the work of [42, 47]. The advantage of Valsa is the ability of controlling the phase variation.

Table 1. Flowcharts depicting the process of four approximation techniques.

Carlson	Matsuda	Oustaloup	Krishna (CFE)
Start	Start	Start	Start
α: fractional-order $H_0(s) = 1$	ω_{min}: minimum frequency ω_{max}: maximum frequency N: approximation order	ω_{min}: minimum frequency ω_{max}: maximum frequency N: approximation order	α: fractional-order N: No. of iterations
$\alpha = \frac{m}{p}, \quad k = \frac{p-m}{p+m}$	$H(s) = s^\alpha$ $d_0(\omega) = \lvert H(j\omega)\rvert$ $d_i(\omega) = \frac{\omega-\omega_{i-1}}{d_{i-1}(\omega)-d_{i-1}(\omega_{i-1})}, \; i=1,2,\dots,2N$	$\omega_{z,i} = \omega_{min}\left(\frac{\omega_{max}}{\omega_{min}}\right)^{(2i-1-\alpha)/2N}$ $\omega_{p,i} = \omega_{min}\left(\frac{\omega_{max}}{\omega_{min}}\right)^{(2i-1+\alpha)/2N}$	$H(s) = \cfrac{1}{1-\cfrac{\alpha(s-1)}{1+\cfrac{(1+\alpha)(s-1)}{2+\cfrac{(1-\alpha)(s-1)}{3+\cdots}}}}$
$H_i = H_{i-1}(s)\frac{s+k[H_{i-1}(s)]^2}{k\; s+[H_{i-1}(s)]^2}$	$H(s) \approx d_0(\omega_0) + \frac{s-\omega_0}{d_1(\omega_1)+} \frac{s-\omega_1}{d_2(\omega_2)+} \cdots$	$s^\alpha \simeq \frac{\prod_{n=1}^{N}\left(1+\frac{s}{\omega_{z,i}}\right)}{\prod_{i=1}^{N}\left(1+\frac{s}{\omega_{p,i}}\right)}$	End
End	End	End	

Table 2. The magnitude and phase responses of four approximation techniques.

	Carlson	Matsuda	Oustaloup	Krishna (CFE)
Magnitude (N)	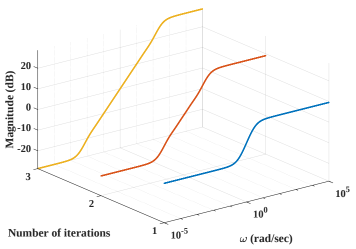	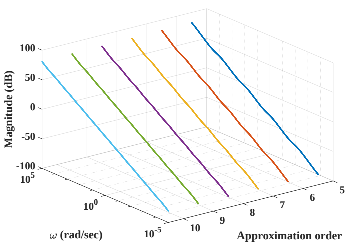	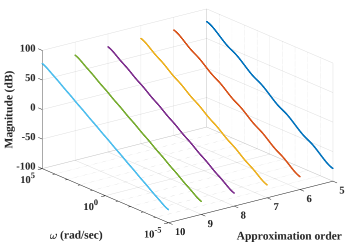	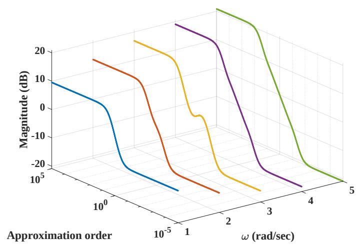
Phase (N)	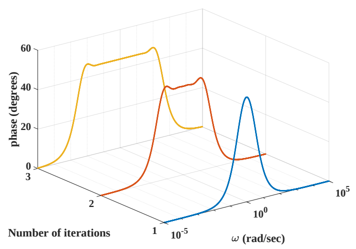	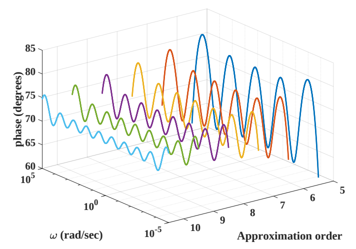	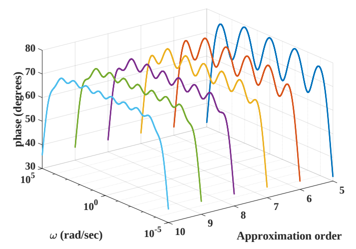	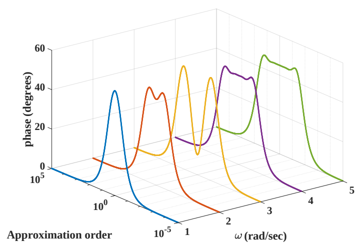
Magnitude (α)	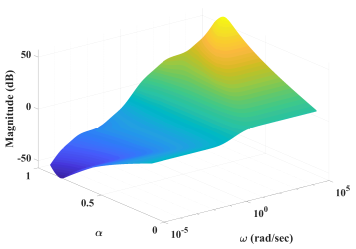	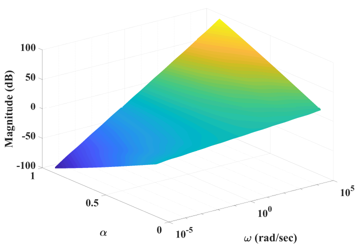	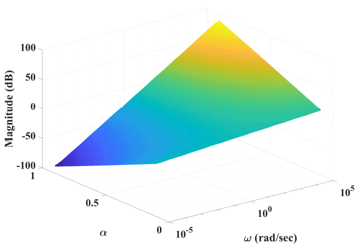	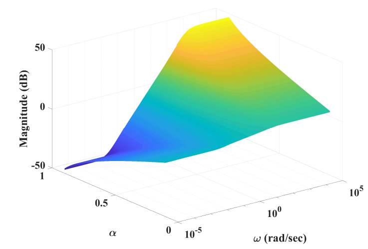
Phase (α)	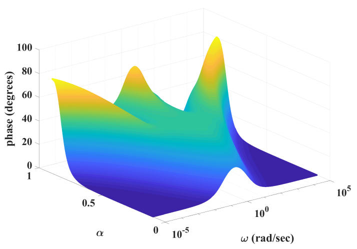	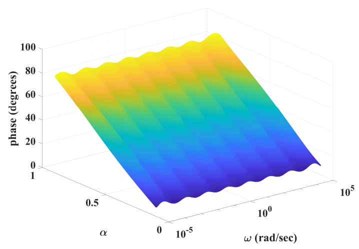	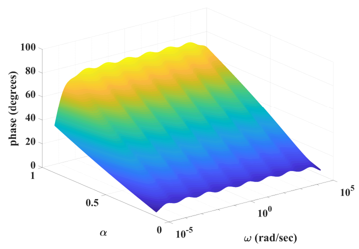	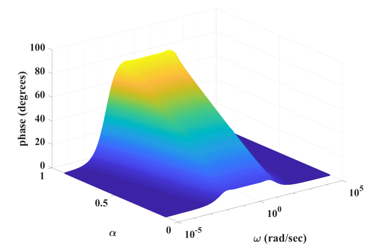

Table 3. Examples of passive emulator circuits for different α values.

Emulators of $\alpha = 0.5$			Emulators of any α.		
	Equations	Diagram		Equations	Diagram
Roy's networks [36]	$R_n = \frac{R}{2n}$, $C_n = \frac{C}{n}$	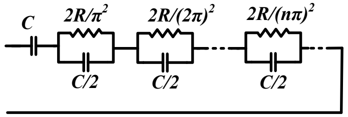	Sugi's networks [37]	$\lambda_i = (R_i C_i)^{-1}$,$\Delta(\ln\lambda) = \ln\lambda_{i+1} - \ln\lambda_i$ $C_n^{\alpha}$is the capacitor in the last branch $R_{i,p} = \left[\frac{C_\alpha C_n^\alpha \ sin\alpha\pi}{\pi}\lambda_i^\alpha \Delta(\ln\lambda)\right]^{-1}$, $C_{i,p} = \frac{C_\alpha C_n^\alpha \ sin\alpha\pi}{\pi}\lambda_i^{\alpha-1}\Delta(\ln\lambda)$	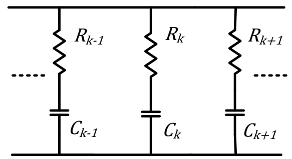
	$R_n = (4n-5)R$, $C_n = (4n-3)C$	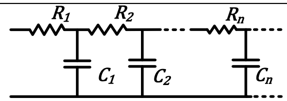		$R_{i,s} = \frac{R_n^\alpha}{C_\alpha}\frac{sin\alpha\pi}{\pi}\lambda_i^{-\alpha}\Delta(\ln\lambda)$, $C_{i,s} = \left[\frac{R_n^\alpha}{C_\alpha}\frac{sin\alpha\pi}{\pi}\lambda_i^{1-\alpha}\Delta(\ln\lambda)\right]^{-1}$	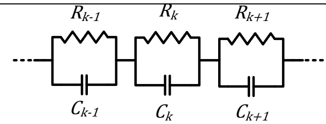
	$R_n = \frac{R}{4n-1}$, $C_n = \frac{C}{4n-3}$	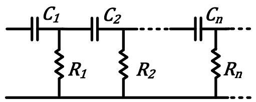			
Nakagawa [46]	$Z = \left(\frac{R}{C}\right)^{0.5} \omega^{-0.5} e^{-\frac{\pi}{4}}$	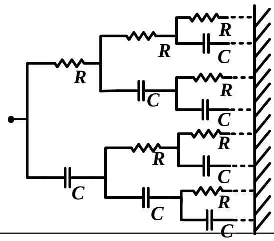	Valsa [38]	$ab \approx \frac{0.24}{1+\Delta\phi}$, $R_m = R_1 a^{m-1}$, $C_m = C_1 b^{m-1}$	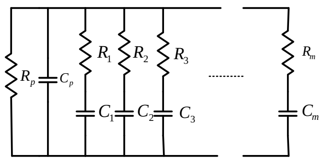
				$R_s = R_1 \frac{a^m}{1-a}$, $C_s = C_1 \frac{1-b}{b}$	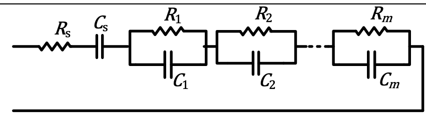

5. STABILITY

Systems can be modeled using differential equations which can be transformed to its counterpart in s-domain using Laplace transform. Checking the system stability is one of the advantages of this transformation. The characteristic equation of a commensurate order fractional order system is $\sum_{k=0}^{N} a_k s^{k\alpha} = 0$. Stability analysis is a discussion about the location of the poles of the characteristic equation and how they affect the time domain response of the system. The response is required to be bounded for any bounded excitation signal.

A new domain was introduced in [48] known as the W-plane. This method is for the rational powers, which can be written in the form $\alpha = k/m$, where k and m are positive integers. Mapping the roots in s-domain to W-plane, requires introducing $W = s^{1/m}$, which makes the mapping process independent on k. The unstable region is at $(|\theta_W| < \pi/2m)$. The stable region is when $(|\theta_W| > pi/2m)$, which includes physical and non-physical roots. Physical roots have correspondence to the s-plane while non-physical ones don't. The stability regions of the W-plane are illustrated in Fig.4.

A general procedure for analyzing the stability of a linear fractional-order differential equation was introduced in [48] for equations on the following form:

$$\sum_{k}^{N} a_k s^{k/m} = \sum_{k=0}^{N} a_k W^k = 0, \tag{9}$$

where $W = s^{k/m}$, and it is a polynomial of order N. The first step is to calculate the roots of

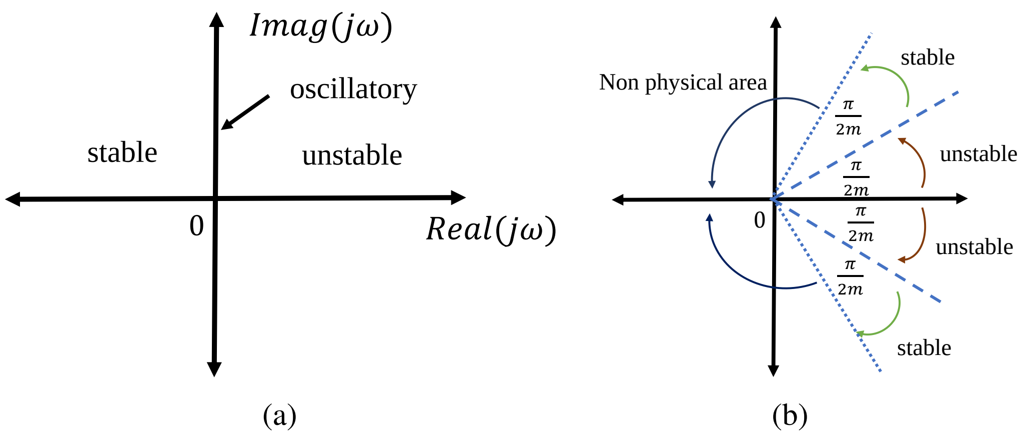

Fig. 4. The stability regions for s^α (a) conventional s-plane at $\alpha = 1$ and (b) the W-plane.

Table 4. Summary for the cases of quadratic equations.

Relation	condition	physical roots
$b < 0$ or ($a^2 \geq b$ and $a < 0$)	unstable independent on α	
$a^2 \geq b$ and $a > 0$ and $b > 0$	stable if $\alpha < 2$	$\alpha < 1$
$a^2 < b$ and $a > 0$ and $b > 0$	stable if and only if $\alpha < \frac{2\delta}{\pi}$, where $\delta = \cos^{-1}(\frac{-a}{\sqrt{b}}) > \frac{\pi}{2}$	$\alpha > \frac{\delta}{\pi}$
$a^2 < b$ and $a < 0$ and $b > 0$	stable if and only if $\alpha < \frac{2\delta}{\pi}$ where $\delta = \cos^{-1}(\frac{-a}{\sqrt{b}}) < \frac{\pi}{2}$	$\alpha > \frac{\delta}{\pi}$

Eq. (9) for given a_k. Then, finding the minimum absolute phase for all roots $|\theta_{Wmin}|$. The stable region is when ($|\theta_{Wmin}| > \pi/2m$), the system is oscillatory at ($|\theta_{Wmin}| = pi/2m$), and it is unstable otherwise. Table 4 shows a summary for the conditions of stability, as well as the physical roots existence condition for the cases as introduced in [48] for system having a characteristic equation of the form $s^{2\alpha} + as^{\alpha} + b = 0$.

For the case of fractional-order characteristic equation, the procedure of [48] is applied and validated for the following cases and summarized in Table 5(1) $s^{2\alpha} + 4s^{\alpha} + 1$ and (2) $s^{2\alpha} - 4s^{\alpha} + 1$, for $0 < \alpha \leq 2$. This representation employs the same $1/m$ to show how the stability is affected by the sign of parameters. The theory of fractional-order stability using W-plane concept [48]is a milestone in this research area. It is one of the grounding concepts and many researchers make use of it in many applications.

6. APPLICATIONS

6.1 Oscillators

Oscillators are widely used in many applications [49] such as: communications (modulation and demodulation), generating clock pulses for microprocessors and micro-controllers, testing and measurements, times and clocks, signal generators, alarms and buzzers. Fractional-order oscillator circuits have two main types according to the nature of the generated signal: sinusoidal and relaxation. Introducing the fractional-order permits an extra design degree of freedom.

The theory of fractional-order sinusoidal oscillators was presented in [50]. It included the design procedure of oscillator of any number of fractance devices. Many fractional-

Table 5. Some stability cases for $s^{2\alpha} \pm s^{\alpha} + 1$ for $(0 < \alpha \leq 2)$

<table>
<tr><th>$\frac{1}{m}$</th><th>$s^{2\alpha} + 4s^{\alpha} + 1$</th><th>$s^{2\alpha} - 4s^{\alpha} + 1$</th></tr>
<tr><td>$\frac{1}{4}$</td><td>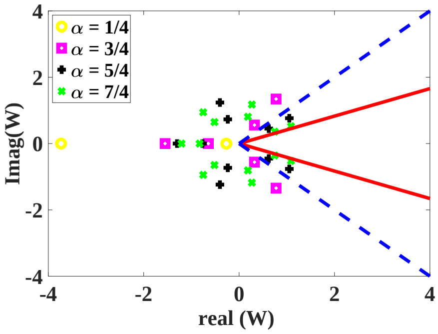</td><td>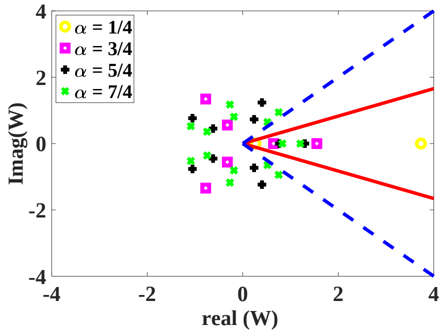</td></tr>
<tr><td>$\frac{1}{2}$</td><td>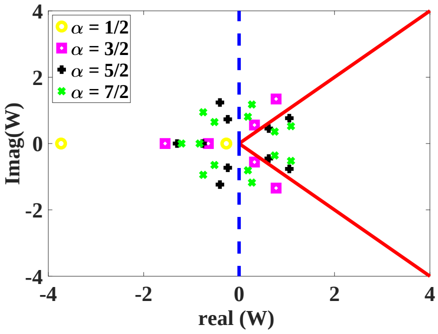</td><td>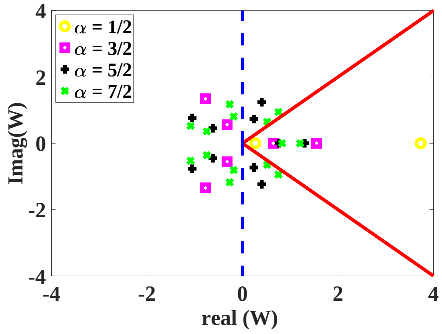</td></tr>
</table>

order oscillators were reported in literature based on the introduced theory such as [51–56]. All possible fractional order oscillators depending on the two-port network concept was proposed in [51,54,57]. Nine possible oscillators were investigated with their mathematical formulas in [58]. Another work showed the design procedure of sinusoidal oscillator using differential voltage current conveyors (DVCC) [59]. A general procedure for designing an oscillator with a specific phase and frequency was also included in [53].

The general state-space formula of the Wien-bridge oscillator shown in Fig. 5a was proposed in [50] and can be written as follows:

$$\begin{pmatrix} D^{\alpha} V_{C1} \\ D^{\beta} V_{C2} \end{pmatrix} = \begin{pmatrix} \frac{a-1}{R_2 C_1} - \frac{1}{R_1 C_1} & \frac{-1}{R_2 C1} \\ \frac{a-1}{R_2 C_2} & \frac{-1}{R_2 C_2} \end{pmatrix} \begin{pmatrix} V_{C1} \\ V_{C2} \end{pmatrix} + \begin{pmatrix} \frac{b}{R_2 C_1} \\ \frac{b}{R_2 C_2} \end{pmatrix}, \tag{10}$$

where α and β are the fractional-order differentiation. The values of (a,b) are characterized as: $(a, b) = (0, V_{sat})$ when $KV_{C1} \geq V_{sat}$, $(K, 0)$ when $-V_{sat} < KV_{C1} < V_{sat}$, and $(0, -V_{sat})$ when $-V_{sat} \geq KV_{C1}$ where V_{sat} is the saturation voltage of the employed operational amplifier and K is the gain factor, and its value is $(1 + \frac{R_3}{R_4})$. Subsequently, the characteristic equation can be written as:

$$s^{\alpha+\beta}+(\frac{K-1}{R_2C_1}-\frac{1}{R_1C_1})s^{\beta}+(\frac{1}{R_2C_2})s^{\alpha}+(\frac{1}{R_1R_2C_1C_2})=0. \tag{11}$$

The following procedure is substituting each s by $j\omega$, then separating the real and imaginary equations. Thus, Eq. (11) turns into:

$$\begin{aligned}\omega^{\alpha+\beta}cos\Big(\frac{(\alpha+\beta)\pi}{2}\Big)-\Big(\frac{K-1}{R_2C_1}-\frac{1}{R_1C_1}\Big)\omega^{\beta}cos\Big(\frac{\beta\pi}{2}\Big)+\Big(\frac{1}{R_2C_2}\Big)\omega^{\alpha}cos\Big(\frac{\alpha\pi}{2}\Big)\\+\Big(\frac{1}{R_1R_2C_1C_2}\Big)=0,\end{aligned} \tag{12}$$

$$\omega^{\beta}sin\Big(\frac{(\alpha+\beta)\pi}{2}\Big)-\Big(\frac{K-1}{R_2C_1}-\frac{1}{R_1C_1}\Big)\omega^{\beta-\alpha}sin\Big(\frac{\beta\pi}{2}\Big)+\Big(\frac{1}{R_2C_2}\Big)\omega^{\alpha}sin\Big(\frac{\alpha\pi}{2}\Big)=0, \tag{13}$$

Sustained sinusoidal oscillation is achieved if solving Eqs. (12,13) results in a real value for oscillation frequency. Moreover, the oscillation condition K is the value at

Table 6. Design parameters of Wien oscillator

case	K	ω	ϕ
$\alpha=\beta\neq 1$	$1+\frac{R_2}{R_1}+\frac{C_1}{C_2}+2\sqrt{\frac{R_2C_1}{R_1C_2}}cos\frac{\alpha\pi}{2}$	$(\frac{1}{R_1R_2C_1C_2})^{\frac{1}{2\alpha}}$	$-tan^{-1}\left(\frac{sin(\frac{\alpha\pi}{2})}{\sqrt{\frac{R_1C_1}{R_2C_2}}+cos(\frac{\alpha\pi}{2})}\right)$
$\alpha=\beta\neq 1$ $R_1=R_2=R$ $C_1=C_2=C$	$3+2cos\frac{\alpha\pi}{2}$	$(\frac{1}{RC})^{\frac{1}{\alpha}}$	$\frac{-\alpha\pi}{2}$
$\alpha=\beta=1$	$1+\frac{R_2}{R_1}+\frac{C_1}{C_2}$	$\sqrt{\frac{1}{R_1R_2C_1C_2}}$	$-tan^{-1}\sqrt{\frac{R_2C_2}{R_1C_1}}$

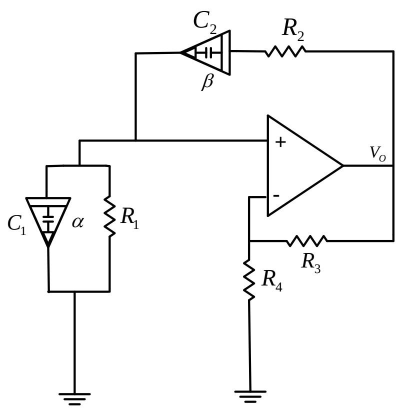

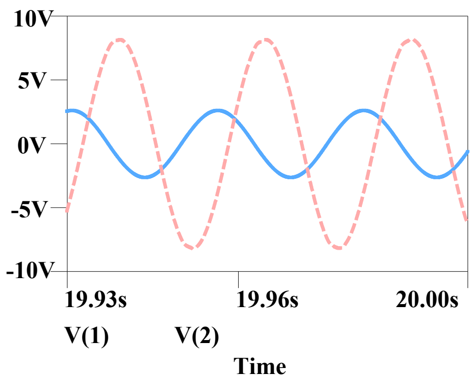

Fig. 5. (a) Wien-bridge oscillator , and (b) Simulation results.

which this real solution exists. This solution scheme starts by excluding the term K from the two formulas of Eqs. (12,13). Consequently, the resultant equation contains only one unknown, the oscillation frequency (ω_{osc}). Due to the difficulty of having closed formulas for the oscillation condition and frequency, some special cases are summarized in Table 6.

According to Table 6, The oscillation frequency gets higher values for $\alpha < 1$. For example, the case of equal R, C, and α, the integer order Wien oscillator whose values ($R = 1$ kΩ, and $C = 100$ nF), has oscillation frequency $\omega = 10$ krad/sec. In the case of employing fractional-order capacitor, utilizing the same components' values despite of the order $\alpha = 0.8$, the resultant frequency is 100 krad/sec, which is 10 times the integer order case. The simulation of this fractional-order case is depicted in Fig. 5b, where the dotted and solid lines are V_{c_1} and V_{c_2}, respectively. Moreover, the phase difference is more controllable in case of fractional-order oscillator as shown in Table 6.

6.2 Filters

The first systematic analysis of fractional order filters was introduced in [60, 61], then many studies followed. The fractional-step Tow-Thomas filter was studied in [62] where the filter topology was generalized to realize band-pass and low-pass filters based on CFE approximation. The detailed analysis of the fractional order Butterworth filter was carried out in [63]. Also, the least square optimization algorithm was used in [64] to approximate the stop-band behavior of fractional order inverse Chebyshev filter. In [21], steps for the realization of fractional-order complex Chebyshev filter were introduced. In [65], the fractional order low-pass, band-pass and high-pass inverse filters were investigated using different approximation techniques. A design procedure for the fractional order Chebyhshev filter having the same poles as the integer order ones was presented in [66]. Fractional-order filters have an extra degree of freedom compared to the conventional ones.

There are some critical frequencies to be calculated for fractional order filters:

- Cutoff(half power) frequency (ω_c): at which the power drops to half the pass band

Table 7. Important frequencies of FO BP filter.

$\omega =$	$\lvert T(j\omega)\rvert$	$\angle T(j\omega)$
0	0	$\frac{\pi}{2}$
ω_o	$\frac{ba^{\beta/\alpha}}{2a\quad(\frac{\alpha\pi}{4})}$	$\frac{\beta\pi}{2}-\frac{\alpha\pi}{4}$
at ∞	$b\omega^{(\beta-\alpha)}$	$\frac{(\beta-\alpha)\pi}{2}$
ω_m	$\frac{d}{asin(\frac{\alpha\pi}{2})}$	$\frac{(1-\alpha)\pi}{2}$
ω_h	$\frac{d}{a\sqrt{2}}$	$tan^{-1}\left(\frac{sin(\frac{\alpha\pi}{2})}{2cos(\frac{\alpha\pi}{2})+\sqrt{1+cos^2(\frac{\alpha\pi}{2})}}\right)$
ω_{rp}	$\frac{d}{a}cot(\frac{\alpha\pi}{2})$	$\frac{\pi}{2}$

$$|T(j\omega_c)| = \frac{|T(j\omega_{\text{pass band},a,b,\alpha})|}{\sqrt{2}}.$$

- Maximum frequency (ω_m): at which the magnitude has a maximum and it is obtained by solving $\frac{d}{d\omega}|T(j\omega)|_{\omega=\omega_h} = 0$, and it can be solved for a certain maximum value.
- Right phase frequency (ω_{rp}): at which the phase $\angle T(j\omega_{rp}) = \pm\frac{\pi}{2}$, and the transfer function is pure imaginary.

An example of simple fractional-order Band Pass Filter (BPF) of the following transfer function has the magnitude response shown in Fig. 6:$T_1(s) = \frac{bs^{\beta}}{s^{\alpha}+a}$. Some important frequency values are summarized on Table 7. In case of $\beta < \alpha$, $\lim_{\omega\to\infty}|T(j\omega)| = 0$. Therefore, the filter acts as a Band Pass Filter. The other case of $\beta = \alpha$ leads to $\lim_{\omega\to\infty}|T(j\omega)| = b$. Thus, the filter develops into a High Pass Filter. In case of $\beta = \alpha = 2$, the center frequency ω_o equals to the maxima frequency. Figure 6 depicts this idea for an example of BPF of equal a and b. The three aforementioned cases are characterized for constant $\alpha = 0.9$ and three different β values at $(B = 0, \alpha/2, \alpha)$.

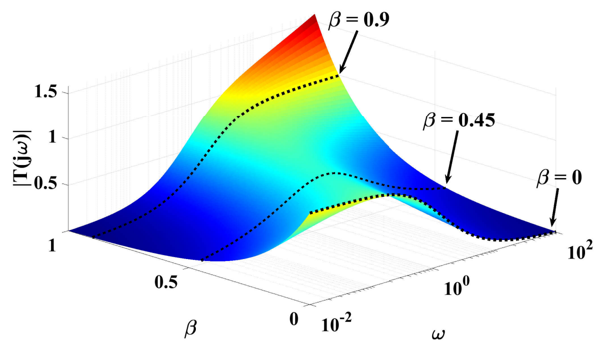

Fig. 6. Example of fractional-order simple fractional BPF.

6.3 Bio-impedance

Bio-impedance is the biological tissue resistance to an applied electrical excitation as shown in Fig. 7 [30]. It is mainly affected by the cell shape and the structure of its membrane [67]. Measuring bio-impedance is a vital indication for any change in cells' structure. It has many applications in different areas such as in medicine [68]. Moreover, it is employed in food industries, to evaluate the state of the tested item. Measuring the maturity or estimating lifespan for storage purposes of fruits and vegetables using the electrical impedance characteristics as achieved in [69]. Moreover, it is employed in monitoring the effects of drying and freezing/thawing treatments on eggplants [70].

The application of bio-impedance rely on the electrical modeling of the tissue cell. There are many introduced models in the literature trying to emulate the most real response. The circuit elements in each topology mimics a component of the tissue cell. The fractional-order based models showed more accurate results compared to its integer counterparts [30, 71]. Table 8 shows a summary of some fractional-order circuit models the tissue cell.

The single dispersion model was employed in many applications such as assessing the quality of stored red blood suspension [68]. Measuring the maturity or estimating lifespan for storage purposes of fruits and vegetables using the electrical impedance characteristics is achieved in [69, 72]. The double dispersion Cole model is found in many applications such as the characterization of intestinal tissue excised from sheep [73]. The age-related

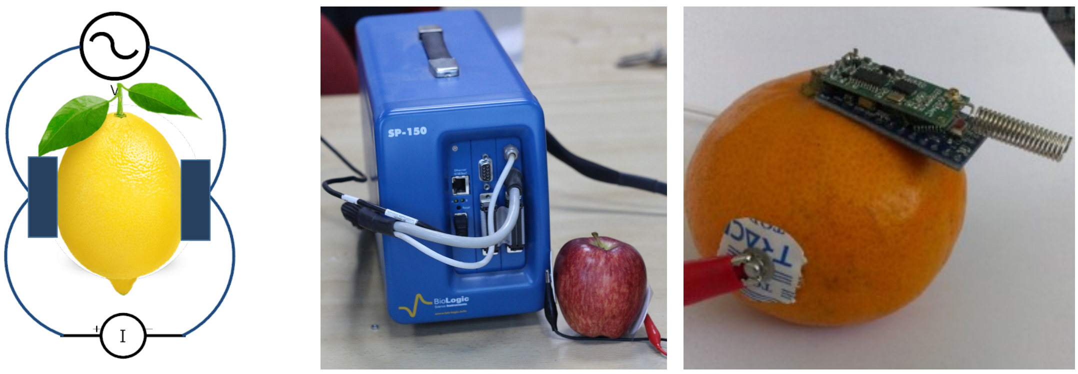

(a) (b) (c)

Fig. 7. (a) Bio-impedance measurement schematic. (b) $SP150$ impedance analyzer experimental setup. (c) Portable impedance analyzer.

Table 8. Examples of fractional-order bio-impedance models.

Model Name	Circuit Model	Nyquist Fit [30]	Best Parameters [30]
Single dispersion [75]	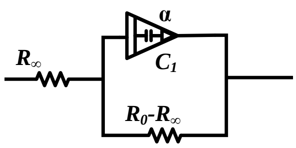	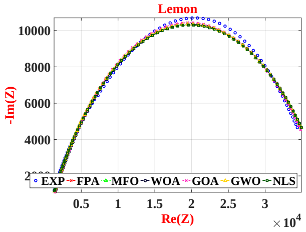	$R_0 = 3.89510^4\Omega$ $R_\infty = 544.4\Omega$ $C = 1.005710^{-7}F \cdot sec^{\alpha-1}$ $\alpha = 0.629$
Simplified Hayden [71]	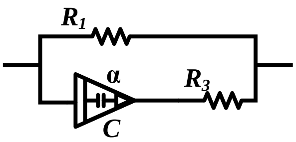	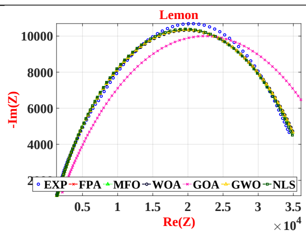	$R_1 = 3.89510^4\Omega$ $R_3 = 552.1\Omega$ $C = 97.7810^{-7}F \cdot sec^{\alpha-1}$ $\alpha = 0.629$
Double shell [71]	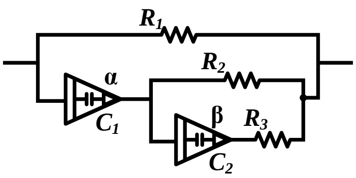	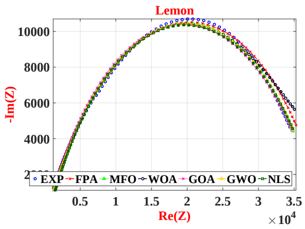	$R_1 = 71.55k\Omega$ $R_2 = 161k\Omega$ $R_3 = 181k\Omega$ $C_1 = 1.465510^{-4}F \cdot sec^{\alpha-1}$ $C_2 = 1.8810^{-4}F \cdot sec^{\beta-1}$ $\alpha = 0.656$ $\beta = 0.74$

changes of dentine was investigated for potential nondestructive dental tests in [74]. The fractional-order simplified Hayden and double shell models were proposed recently [71].

Electro-chemical Impedance Spectroscopy (EIS) is the most widely known measuring methodology. The basic setup and connections of EIS are depicted in Fig. 7. It involves exposing the targeted tissue as a black box to a wide range of frequencies. Then, optimization algorithms are employed to fit the results to the best model [76]. There are many measuring techniques such as transient time measurements, where a step function of voltage is applied to the targeted impedance, then applying Fast Fourier Transform (FFT) on the the resultant current [77].

Most commercial impedance analyzers such as the $SP150$ (see Fig. 7) and their associated programs have built-in function that allows the user to fit the measurement either to well-known impedance models or even a user-defined one. The common fitting technique is the complex nonlinear least squares technique (CNLS). Although it might be satisfactory in some cases, when the model gets more complicated it gives un-acceptable fits. This is due to the fact that CNLS is a gradient based optimization technique, also known as deterministic technique, which is prone to local minima and measurement outliers. Recently, researchers used meta-heuristic optimization algorithms to identify the parameters of many bio-impedance models. They mimic the searching/hunting behavior of animals in nature in order to find the global optimal solution and are less likely to fall into local minima of the optimization problem due to a balance between intensification and diversification of their search agents. Examples of these algorithms include flower pollination algorithm (FPA), grey wolf optimizer (GWO), moth flame optimizer (MFO), grasshopper optimization algorithm (GOA), whale optimization algorithm (WOA).

Three items must be defined in any optimization problem. Theses items are the search vector, the objective function, and the feasible region. In parameter estimation of bio-impedance models, the search vector has a dimension equal to the number parameters to be identified. For example, in case of single dispersion model, the parameters are R_0, C_α, R_∞, and α, so the dimension of the search vector is 4 and is written as $X = [R_0, C_\alpha, R_\infty, \alpha]$. For the objective function, the common one in literature is the some of absolute error given as $SAE = \sum_{i=1}^{M} |Z_i - \tilde{Z}_i|$, where M is the number of data-points, Z_i is the measured complex impedance at frequency ω_i, $\tilde{Z}_i$ is the estimated impedance at frequency ω_i and is calculated from the model formula as $Z(s) = R_\infty + \frac{R_0 - R_\infty}{1+s^\alpha(R_0-R_\infty)C}$.

The feasible region is described through implying constraints on the search vector variables. For example, in case of identifying the model parameters of Lemon, the lower limits are defined as $lb = [10k, 1n, 1, 0.4]$, and the upper limits are defined as $ub = [500k, 1\mu, 10k, 1.0]$. The same formulation can be made for identifying the fractional order Hayden model and the fractional order double-shell model .

When comparing the performance of different meta-heuristic optimization techniques at solving this problem, three main aspects are defined which are accuracy and consistency, objective function final value, and run-time. The accuracy and consistency means the algorithm achieves almost the same results in each independent run. This is measured from the standard deviation of the results of all independent runs made on the same PC. Lower standard deviation means more accurate and consistent algorithm. It was found that FPA is the most consistent in solving this problem. The run-time needed to get the results depends on two main factors, the convergence speed of the algorithm, and the number of calculations per iteration of the algorithm. Unfortunately, usually meta-heuristic optimization techniques takes longer run-times than gradient based algorithms like CNLS and nonlinear least squares (NLS). This means that there is a trade-off between speed and accuracy in this case. The fit results of identifying the bioimpedance parameters of lemon are shown in Table 8.

6.4 DC-DC Converters

In the ideal case, the energy storage elements are lossless and the efficiency of the system is 100%. However, in practicality, the coils have many types of losses. One of these types is the hysteresis loss which results from the use of ferromagnetic cores that retain magnetization and increases both the inductance and losses which were found to be frequency dependent [78]. This is due to the fact that the coils in power converter operate near their magnetic saturation levels where the magnetic losses and skin effect can not be modeled linearly. Fractional order models can be used here to provide an accurate emulation of such losses associated with inductors inside DC-DC converter operating conditions.

The circuit schematic of the Buck DC-DC converter topology is illustrated in Fig. 8. The converter has two switches, one inductor and one capacitor. Switch $S1$ is usually is the active bidirectional switch while switch $S2$ is the passive uni-directional switch. In continuous conduction mode (CCM), the circuit has only two states: when $S1$ is on and $S2$ is off, and when $S1$ is off and $S2$ is on. In discontinuous conduction mode (DCM), another state is added which is both switches are off. Analysis of fractional order DC-DC converter in literature is either concerned with the steady state behavior [79] or the transient behavior [80].

The generalized procedure for steady state analysis of fractional order DC-DC converter in CCM mode can be summarized as follows. Assume that, at steady state, the voltage across the fractional-order inductor is constant during each switching state and changes accordingly between v_1 in the interval $[nT, (n + D)\,T]$ to v_2 in $[(n + D)\,T, (n + 1)\,T]$

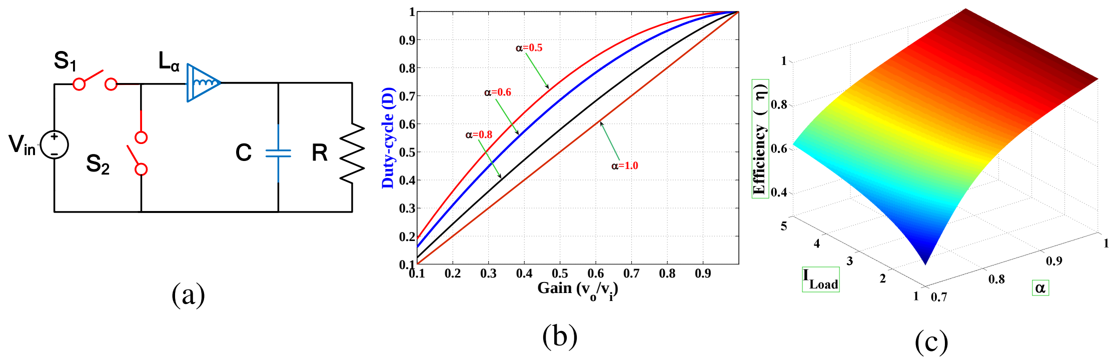

Fig. 8. (a) Buck converter. (b) Gain vs duty cycle. (c) The efficiency.

where $n \in Z^{+}$. Where $v_1$is the voltage across the inductor when the active switch is ON and the passive switch is OFF (diode is reverse biased), while v_2 is the inductor voltage when the active switch is OFF and the passive switch is ON (diode is forward biased). Another assumption is that the capacitor ripple voltage is negligible. Also, assume that the inductor current has stabilized which means no rising or falling in its average value, so the inductor current value at $t = nT$ will be the same and is equal to $i_{L2}(T, \alpha)$. For simplicity, we will write the equations of the current waveforms in the first period ($n = 0$). Therefore, the current $i_L(t, \alpha)$ is given by: in the interval $t \in [0, DT]$

$$i_{L1}(t, \alpha) = i_{L2}(T, \alpha) + \frac{1}{L\Gamma(\alpha)} \int_0^t (t-\tau)^{\alpha-1} v_1 d\tau = i_{L2}(T,\alpha) + \frac{v_1 t^{\alpha}}{L\Gamma(\alpha+1)}. \tag{14}$$

In the interval $t \in [DT, T]$

$$i_{L2}(t,\alpha) = i_{L2}(T,\alpha) + \frac{1}{L\Gamma(\alpha+1)} \left(v_1 t^{\alpha} + (v_2 - v_1)(t - DT)^{\alpha}\right). \tag{15}$$

By setting $t = T$ in equation (15), the relation between v_1 and v_2 becomes:

$$v_1 T^{\alpha} + (v_2 - v_1)(T - DT)^{\alpha} = 0 \longrightarrow \frac{v_1}{v_2} = \frac{(1-D)^{\alpha}}{(1-D)^{\alpha} - 1} \longrightarrow D = 1 - \left(\frac{v_1}{v_1 - v_2}\right)^{\frac{1}{\alpha}}. \tag{16}$$

which is the fractional equivalent of the inductor volt-second balance.

In case of the fractional order buck converter, by substituting v_1 and v_2 with $(v_{\text{in}} - v_{\text{out}})$ and $(-v_{\text{out}})$, respectively in the previous equation, the duty cycle D and voltage gain G

can be written as:

$$D = 1 - \left(\frac{v_{in} - v_{out}}{v_{in}}\right)^{\frac{1}{\alpha}}, G = \frac{v_o}{v_{in}} = 1 - (1 - D)^{\alpha}. \tag{17}$$

Note that when $D = 1$, then $v_{out} = v_{in}$ for any value of α. It is evident that D increases for smaller values of α to compensate for the inductor fractional losses. The relation between the gain G and the duty cycle D at different values of the fractional order α is shown in Fig. 8b.

The efficiency is calculated as the ratio between average energy dispatched to the load and average energy taken out of the source and assuming the steady state operation condition which means that the input and output voltages variations are negligible. Therefore, the average power efficiency in this case is given as [79]:

$$\eta = \frac{E_{out}}{E_{in}} = \frac{D}{(1 - (1 - D)^{\alpha})\, i_{load}} \left[i_{load} - \frac{v_{in} T^{\alpha}}{L\Gamma(\alpha + 2)} (1 - D)^{\alpha} (D^{\alpha} - D)\right], \tag{18}$$

where i_{load} is the average load current. Figure 8c shows the efficiency of the buck converter at as a function of α and i_{load}. It is evident that the efficiency degrades with decreasing α and i_{load}.

7. CONCLUSION

A literature survey was presented about the fractional calculus fundamentals, integer-order approximations of fractional-order transfer functions, fractional-order element realization, fractional-order circuits and applications, and stability analyses of fractional-order linear systems. The investigated applications included fractional-order oscillators, filters, passive emulators, bio-impedance modeling and DC-DC converters. In most cases, the fractional-order models are more accurate than the integer-order ones. All fractional operators consider the entire history of the process being considered, thus being able to model the non-local and distributed effects often encountered in natural and technical phenomena. The extra degrees of freedom give different design alternatives due to the fractional-order parameters. Fractional-order models provide an improved description of observed bio-impedance behavior. Additionally, the fractional-order enhanced the model of DC-DC converters by incorporating the effect of frequency-dependent inductor loss.

DECLARATION OF CONFLICT OF INTERESTS

The authors have declared no conflict of interests.

ACKNOWLEDGMENTS

Authors would like to thank Science and Technology Development Fund (STDF) for funding the project # 25977 and Nile University for facilitating all procedures required to complete this study.

REFERENCES

1. Machado, J.A.T., and Kiryakova, V. “Recent History of the Fractional Calculus: Data and Statistics”, In A. Kochubei, and Y. Luchko, editors, Basic Theory, pp. 1–22. De Gruyter, 2019.
2. Podlubny, I. Fractional Differential Equations: An Introduction to Fractional Derivatives, Fractional Differential Equations, to Methods of Their Solution and Some of Their Applications. Academic press, 1998.
3. Kapoulea, S., Bizonis, V., Bertsias, P., Psychalinos, C., Elwakil, A., and Petráš, I. “Reduced Active Components Count Electronically Adjustable Fractional-Order Controllers: Two Design Examples”, Electronics, Vol. 9, No. 1, p. 63, 2020.
4. Sun, G., Wu, L., Kuang, Z., Ma, Z., and Liu, J. “Practical Tracking Control of Linear Motor via Fractional-Order Sliding Mode”, Automatica, Vol. 94, pp. 221–235, 2018.
5. Dimeas, I., Petras, I., and Psychalinos, C. “New Analog Implementation Technique for Fractional-Order Controller: a DC Motor Control”, AEU-International Journal of Electronics and Communications, Vol. 78, pp. 192–200, 2017.
6. Tolba, M.F., AboAlNaga, B.M., Said, L.A., Madian, A.H., and Radwan, A.G. “Fractional Order Integrator/Differentiator: FPGA Implementation and FOPID Controller Application”, AEU-International Journal of Electronics and Communications, Vol. 98, pp. 220–229, 2019.
7. Tolba, M.F., Saleh, H., Mohammad, B., Al-Qutayri, M., Elwakil, A.S., and Radwan, A.G. “Enhanced FPGA Realization of the Fractional-Order Derivative and Application to a Variable-Order Chaotic System”, Nonlinear Dynamics, 2020.
8. Li, P., Xu, J., Mou, J., and Yang, F. “Fractional-Order 4D Hyperchaotic Memristive System and Application in Color Image Encryption”, EURASIP Journal on Image and Video Processing, Vol. 2019, No. 1, p. 22, 2019.

9. Soliman, N.S., Tolba, M.F., Said, L.A., Madian, A.H., and Radwan, A.G. “Fractional X-Shape Controllable Multi-scroll Attractor with Parameter Effect and FPGA Automatic Design Tool Software”, Chaos, Solitons & Fractals, Vol. 126, pp. 292–307, 2019.
10. Tolba, M.F., AbdelAty, A.M., Said, L.A., Madian, A.H., and Radwan, A.G. “FPGA Implementation of Fractional-Order Chaotic Systems”, In Fractional Order Systems, pp. 33–62. Elsevier, 2018.
11. Tolba, M.F., AbdelAty, A.M., Soliman, N.S., Said, L.A., Madian, A.H., Azar, A.T., and Radwan, A.G. “FPGA Implementation of Two Fractional Order Chaotic Systems”, AEU-International Journal of Electronics and Communications, Vol. 78, pp. 162–172, 2017.
12. Boulkroune, A., Bouzeriba, A., and Bouden, T. “Fuzzy Generalized Projective Synchronization of Incommensurate Fractional-Order Chaotic Systems”, Neurocomputing, Vol. 173, pp. 606–614, 2016.
13. Ismail, S.M., Said, L.A., Radwan, A.G., Madian, A.H., and Abu-ElYazeed, M.F. “A Novel Image Encryption System Merging Fractional-Order Edge Detection and Generalized Chaotic Maps”, Signal Processing, Vol. 167, p. 107280, 2020.
14. Liu, Z., and Xia, T. “Novel Two Dimensional Fractional-Order Discrete Chaotic Map and its Application to Image Encryption”, Applied Computing and Informatics, Vol. 14, No. 2, pp. 177–185, 2018.
15. Ismail, S.M., Said, L.A., Rezk, A.A., Radwan, A.G., Madian, A.H., Abu-ElYazeed, M.F., and Soliman, A.M. “Biomedical image encryption based on double-humped and fractional logistic maps”, In Modern Circuits and Systems Technologies (MOCAST), 2017 6^{th} International Conference on, pp. 1–4. IEEE, 2017.
16. Ismail, S.M., Said, L.A., Rezk, A.A., Radwan, A.G., Madian, A.H., Abu-Elyazeed, M.F., and Soliman, A.M. “Generalized Fractional Logistic Map Encryption System Based on FPGA”, AEU-International Journal of Electronics and Communications, Vol. 80, pp. 114–126, 2017.
17. Allagui, A., Alnaqbi, H., Elwakil, A.S., Said, Z., Hachicha, A.A., Wang, C., and Abdelkareem, M.A. “Fractional-Order Electric Double-Layer Capacitors with Tunable Low-frequency Impedance Phase Angle and Energy Storage Capabilities”, Applied Physics Letters, Vol. 116, No. 1, p. 013902, 2020.
18. Allagui, A., Freeborn, T.J., Elwakil, A.S., Fouda, M.E., Maundy, B.J., Radwan, A.G., Said, Z., and Abdelkareem, M.A. “Review of Fractional-Order Electrical Characterization of Supercapacitors”, Journal of Power Sources, Vol. 400, pp. 457–467, 2018.
19. Fouda, M., Elwakil, A., Radwan, A., and Allagui, A. “Power and Energy aAnalysis of Fractional-Order Electrical Energy Storage Devices”, Energy, Vol. 111, pp. 785 – 792, 2016.
20. Prasad, D., Kumar, M., and Akram, M.W. “Current mode fractional order filters using VDTAs with Grounded capacitors”, International Journal of Electronics and Telecommunications, Vol. 65, No. 1, pp. 11–17, 2019.

21. AbdelAty, A.M., Soltan, A., Ahmed, W.A., and Radwan, A.G. “On the Analysis and Design of Fractional-Order Chebyshev Complex Filter”, Circuits, Systems, and Signal Processing, Vol. 37, No. 3, pp. 915–938, 2017.
22. Khalil, N.A., Said, L.A., Radwan, A.G., and Soliman, A.M. “Generalized two-port network based fractional order filters”, AEU-International Journal of Electronics and Communications, Vol. 104, pp. 128–146, 2019.
23. Hamed, E.M., AbdelAty, A.M., Said, L.A., and Radwan, A.G. “Effect of Different aApproximation Techniques on Fractional-Order KHN Filter Design”, Circuits, Systems, and Signal Processing, Vol. 37, No. 12, pp. 5222–5252, 2018.
24. Radwan, A.G., and Fouda, M.E. “Optimization of Fractional-Order RLC Filters”, Circuits, Systems, and Signal Processing, Vol. 32, No. 5, pp. 2097–2118, 2013.
25. Said, L.A., Biswas, K., and Radwan, A.G. “Chapter 12 - Fractional-Order Filter Design”, In A.T. Azar, A.G. Radwan, and S. Vaidyanathan, editors, Fractional Order Systems, Advances in Nonlinear Dynamics and Chaos (ANDC), pp. 357 – 382. Academic Press, 2018.
26. Hanna, M.T. “A Discrete Fractional Fourier Transform Based on Orthonormalized Mcclelian-Parks Eigenvectors”, Journal of Engineering and Applied Science, Vol. 51, No. 1, pp. 11–30, 2004.
27. Bertsias, P., Psychalinos, C., Elwakil, A., Safari, L., and Minaei, S. “Design and Application Examples of CMOS Fractional-Order Differentiators and Integrators”, Microelectronics Journal, Vol. 83, pp. 155–167, 2019.
28. Fu, B., and Freeborn, T.J. “Residual impedance effect on emulated bioimpedance measurements using Keysight E4990A precision impedance analyzer”, Measurement, Vol. 134, pp. 468–479, 2019.
29. Yousri, D., AbdelAty, A.M., Said, L.A., Elwakil, A., Maundy, B., and Radwan, A.G. “Chaotic Flower Pollination and Grey Wolf Algorithms for parameter extraction of bio-impedance models”, Applied Soft Computing, Vol. 75, pp. 750 – 774, 2019.
30. Yousri, D., AbdelAty, A.M., Said, L.A., and Radwan, A.G. “Biologically Inspired Optimization Algorithms for Fractional-Order Bioimpedance Models Parameters Extraction”, In Fractional Order Systems, pp. 125–162. Elsevier, 2018.
31. Teodoro, G.S., Machado, J.T., and de Oliveira, E.C. “A Review of Definitions of Fractional Derivatives and Other Operators”, Journal of Computational Physics, Vol. 388, pp. 195 – 208, 2019.
32. Valério, D., and Sà da Costa, J.S. “Introduction to Single-Input, Single-Output Fractional Control”, IET Control Theory Applications, Vol. 5, No. 8, pp. 1033–1057, 2011.
33. Ogata, K., and Yang, Y. Modern control engineering, Vol. 4. Prentice hall India, 2002.
34. Vinagre, B., Podlubny, I., Hernandez, A., and Feliu, V. “Some Approximations of Fractional Order Operators Used in Control Theory and Applications”, Fractional Calculus and Applied Analysis, Vol. 3, No. 3, pp. 231–248, 2000.

35. Elwakil, A.S. “Fractional-order circuits and systems: An emerging interdisciplinary research area”, IEEE Circuits and Systems Magazine, Vol. 10, No. 4, pp. 40–50, 2010.
36. Roy, S. “On the realization of a constant-argument immittance or fractional operator”, IEEE Transactions on Circuit Theory, Vol. 14, No. 3, pp. 264–274, 1967.
37. Sugi, M., Hirano, Y., Miura, Y.F., and Saito, K. “Simulation of fractal immittance by analog circuits: An approach to the optimized circuits”, IEICE Trans. Fundam. Electron. Commun. Comput. Sci., Vol. E82-A, No. 8, pp. 1627–1635, 1999.
38. Valsa, J., Dvorak, P., and Friedl, M. “Network model of the CPE”, Radioengineering, Vol. 20, No. 3, pp. 619–626, 2011.
39. Tsirimokou, G., Psychalinos, C., Elwakil, A., and Salama, K. “Experimental verification of on-chip CMOS fractional-order capacitor emulators”, Electronics Letters, Vol. 52, No. 15, pp. 1298–1300, 2016.
40. Bertsias, P., Psychalinos, C., Elwakil, A., and Maundy, B. “Current-Mode Capacitorless Integrators and Differentiators for Implementing Emulators of Fractional-Order Elements”, AEU-International Journal of Electronics and Communications, Vol. 80, pp. 94–103, 2017.
41. Tsirimokou, G., Kartci, A., Koton, J., Herencsar, N., and Psychalinos, C. “Comparative Study of Discrete Component Realizations of Fractional-Order Capacitor and Inductor Active Emulators”, Journal of Circuits, Systems and Computers, p. 1850170, 2018.
42. Morrison, R. “RC constant-argument driving-point admittances”, IRE Transactions on Circuit Theory, Vol. 6, No. 3, pp. 310–317, 1959.
43. Elshurafa, A.M., Almadhoun, M.N., Salama, K., and Alshareef, H. “Microscale electrostatic fractional capacitors using reduced graphene oxide percolated polymer composites”, Applied Physics Letters, Vol. 102, No. 23, p. 232901, 2013.
44. Valsa, J., and Vlach, J. “RC models of a constant phase element”, International Journal of Circuit Theory and Applications, Vol. 41, No. 1, pp. 59–67, 2013.
45. Duffett-Smith, P. “Synthesis of lumped element, distributed, and planar filters”, Journal of Atmospheric and Terrestrial Physics, Vol. 52, No. 9, pp. 811–812, 1990.
46. Nakagawa, M., and Sorimachi, K. “Basic characteristics of a fractance device”, IEICE Transactions on Fundamentals of Electronics, Communications and Computer Sciences, Vol. 75, No. 12, pp. 1814–1819, 1992.
47. Machado, J. “Discrete-time fractional-order controllers”, Fractional Calculus and Applied Analysis, Vol. 4, pp. 47–66, 2001.
48. Radwan, A.G., Soliman, A., Elwakil, A.S., and Sedeek, A. “On the Stability of Linear Systems with Fractional-Order Elements”, Chaos, Solitons & Fractals, Vol. 40, No. 5, pp. 2317–2328, 2009.
49. Bell, D.A. Electronic Instrumentation and Measurements. Englewood Cliffs, NJ: Regents/Prentice Hall,, 2011.
50. Radwan, A.G., Elwakil, A.S., and Soliman, A.M. “Fractional-order sinusoidal oscillators: design procedure and practical examples”, IEEE Transactions on Circuits and Systems I: Regular Papers, Vol. 55, No. 7, pp. 2051–2063, 2008.

51. Said, L.A., Radwan, A.G., Madian, A.H., and Soliman, A.M. "Two-port two impedances fractional order oscillators", Microelectronics Journal, Vol. 55, pp. 40–52, 2016.
52. Said, L.A., Radwan, A.G., Madian, A.H., and Soliman, A.M. "Generalized family of fractional-order oscillators based on single CFOA and RC network", In Modern Circuits and Systems Technologies (MOCAST), 2017 6^{th} International Conference on, pp. 1–4. IEEE, 2017.
53. Said, L.A., Radwan, A.G., Madian, A.H., and Soliman, A.M. "Three fractional-order-capacitors-based oscillators with controllable phase and frequency", Journal of Circuits, Systems and Computers, Vol. 26, No. 10, p. 1750160, 2017.
54. Said, L.A., Radwan, A.G., Madian, A.H., and Soliman, A.M. "Survey on Two-Port Network-Based Fractional-Order Oscillators", In Fractional Order Systems, pp. 305–327. Elsevier, 2018.
55. Fouda, M.E., Soltan, A., Radwan, A.G., and Soliman, A.M. "Fractional-order multi-phase oscillators design and analysis suitable for higher-order PSK applications", Analog Integrated Circuits and Signal Processing, Vol. 87, No. 2, pp. 301–312, 2016.
56. Said, L.A., Radwan, A.G., Madian, A.H., and Soliman, A.M. "Fractional-Order Oscillator Based on Single CCII", In 2016 39th International Conference on Telecommunications and Signal Processing (TSP), pp. 603–606, 2016.
57. Said, L.A., Radwan, A.G., Madian, A.H., and Soliman, A.M. "Fractional-order inverting and non-inverting filters based on CFOA", In Telecommunications and Signal Processing (TSP), 2016 39th International Conference on, pp. 599–602. IEEE, 2016.
58. Said, L.A., Radwan, A.G., Madian, A.H., and Soliman, A.M. "Fractional Order Oscillator Design Based on Two-Port Network", Circuits, Syst. Signal Process., Vol. 35, No. 9, pp. 3086–3112, 2016.
59. Kubánek, D., Khateb, F., Tsirimokou, G., and Psychalinos, C. "Practical Design and Evaluation of Fractional-Order Oscillator Using Differential Voltage Current Conveyors", Circuits, Systems, and Signal Processing, Vol. 35, No. 6, pp. 2003–2016, 2016.
60. Radwan, A.G., Elwakil, A.S., and Soliman, A.M. "On the Generalization of Second-Order Filters to the Fractional-Order Domain", Journal of Circuits, Systems, and Computers, Vol. 18, No. 02, pp. 361–386, 2009.
61. Radwan, A.G., Soliman, A.M., and Elwakil, A.S. "First-Order Filters Generalized to the Fractional Domain", Journal of Circuits, Systems, and Computers, Vol. 17, No. 01, pp. 55–66, 2008.
62. Freeborn, T.J., Maundy, B., and Elwakil, A. "Fractional-Step Tow-Thomas Biquad Filters", Nonlinear Theory and Its Applications, IEICE, Vol. 3, No. 3, pp. 357–374, 2012.
63. Ali, A.S., Radwan, A.G., and Soliman, A.M. "Fractional Order Butterworth Filter: Active and Passive Realizations", IEEE Journal on Emerging and Selected Topics in Circuits and Systems, Vol. 3, No. 3, pp. 346–354, 2013.

64. Freeborn, T.J., Elwakil, A.S., and Maundy, B. “Approximated Fractional-Order Inverse Chebyshev Lowpass Filters”, Circuits, Systems, and Signal Processing, Vol. 35, No. 6, pp. 1973–1982, 2016.
65. Hamed, E.M., Said, L.A., Madian, A.H., and Radwan, A.G. “On the Approximations of CFOA-Based Fractional-Order Inverse Filters”, Circuits, Systems, and Signal Processing, 2019.
66. AbdelAty, A.M., Soltan, A., Ahmed, W.A., and Radwan, A.G. “Fractional Order Chebyshev-Like Low-Pass Filters Based on Integer Order Poles”, Microelectronics Journal, Vol. 90, pp. 72 – 81, 2019.
67. Yousri, D., AbdelAty, A.M., Said, L.A., AboBakr, A., and Radwan, A.G. “Biological inspired optimization algorithms for cole-impedance parameters identification”, AEU-International Journal of Electronics and Communications, Vol. 78, pp. 79–89, 2017.
68. Sezdi, M., Bayik, M., and Ulgen, Y. “Storage Effects on the Cole-Cole Parameters of Erythrocyte Suspensions”, Physiological Measurement, Vol. 27, No. 7, p. 623, 2006.
69. Jesus, I.S., and Tenreiro Machado, J. “Application of Integer and Fractional Models in Electrochemical Systems”, Mathematical Problems in Engineering, Vol. 2012, 2012.
70. Wu, L., Ogawa, Y., and Tagawa, A. “Electrical Impedance Spectroscopy Analysis of Eggplant Pulp and Effects of Drying and Freezing–Thawing Treatments on its Impedance Characteristics”, Journal of Food Engineering, Vol. 87, No. 2, pp. 274–280, 2008.
71. AboBakr, A., Said, L.A., Madian, A.H., Elwakil, A.S., and Radwan, A.G. “Experimental comparison of integer/fractional-order electrical models of plant”, AEU-International Journal of Electronics and Communications, Vol. 80, pp. 1–9, 2017.
72. Jesus, I.S., Tenreiro Machado, J., and Boaventure Cunha, J. “Fractional Electrical Impedances in Botanical Elements”, Journal of Vibration and Control, Vol. 14, No. 9-10, pp. 1389–1402, 2008.
73. Rigaud, B., Hamzaoui, L., Frikha, M.R., Chauveau, N., and Morucci, J.P. “In Vitro Tissue Characterization and Modelling Using Electrical Impedance Measurements in the 100 Hz-10 MHz Frequency Range”, Physiological Measurement, Vol. 16, No. 3A, pp. A15–A28, 1995.
74. Eldarrat, A.H., Wood, D.J., Kale, G.M., and High, A.S. “Age-Related Changes in AC-Impedance Spectroscopy Studies of Normal Human Dentine”, Journal of Materials Science: Materials in Medicine, Vol. 18, No. 6, pp. 1203–1210, 2007.
75. Cole, K.S., and Cole, R.H. “Dispersion and Absorption in Dielectrics I. Alternating Current Characteristics”, The Journal of Chemical Physics, Vol. 9, No. 4, pp. 341–351, 1941.
76. Al-Ali, A.A., Maundy, B.J., and Elwakil, A.S. Design and Implementation of Portable Impedance Analyzers. Springer, 2019.
77. Macdonald, J.R., and Barsoukov, E. “Impedance Spectroscopy: Theory, Experiment, and Applications”, History, Vol. 1, No. 8, pp. 1–13, 2005.

78. Schäfer, I., Krüger, K., Schafer, I., and Kruger, K. "Modelling of Lossy Coils Using Fractional Derivatives", J. Phys. D. Appl. Phys., Vol. 41, No. 4, p. 45001, 2008.
79. Radwan, A.G., Emira, A.A., AbdelAty, A.M., and Azar, A.T. "Modeling and Analysis of Fractional Order DC-DC Converter", ISA Transactions, Vol. 82, pp. 184 – 199, 2018. Fractional Order Signals, Systems, and Controls: Theory and Application.
80. Jia, Z., and Liu, C. "Fractional-Order Modeling and Simulation of Magnetic Coupled Boost Converter in Continuous Conduction Mode", International Journal of Bifurcation and Chaos, Vol. 28, No. 05, p. 1850061, 2018.

التفاضل الكسرى: تعريفات و تقريبات و تطبيقات هندسية

الفكرة الأساسية فى التفاضل الكسرى هى إمكانية حساب مشتقات و تكاملات من درجات كسرية مما أتاح مزيداً من القدرة على وصف أنظمة معقدة وصفاً محكماً. هذا البحث يقدم وصفاً موجزاً عن التفاضل الكسرى و بعض تطبيقاته. يسرد البحث بعض من التعريفات الأساسية مصحوبة ببعض الأمثلة التوضيحية. يتبع ذلك حديث عن التقريبات و دوائر المحاكاة. كذلك تحتوى على تلخيص لنظرية إتزان الأنظمة الكسرية. يتبع ذلك وصف موجز لأربعة تطبيقات هندسية. المذبذبات كسرية الدرجة التى تتيح مزيداً من التحكم فى أطوار الموجات المتولدة كما تسهل الحصول على ترددات عالية. المرشحات كسرية الدرجة التى أتاحت مزيداً من الدقة فى حسابات خصائص المرشح. دراسة نماذج المقاومة الحيوية للأنسجة، التى تُمكنا من إجراء العديد من القياسات الدقيقة على الفواكه و الخضروات. محولات الجهد الثابت التى تتيح تقريبات أفضل فى حسابات تحويل القوى بالاستعانة بحساب فواقد الطاقة المعتمدة على الترددات.